Dynamic-Mechanical and Thermal Characterization of Polypropylene/Ethylene–Octene Copolymer Blend

Smita Mohanty,[1] Sanjay K. Nayak[2]

[1]*Central Institute of Plastics Engineering and Technology, Chennai 600 032, India*
[2]*Central Institute of Plastics Engineering and Technology, Bhubaneswar 751 024, India*

Received 14 September 2005; accepted 26 November 2006
DOI 10.1002/app.25941
Published online 5 March 2007 in Wiley InterScience (www.interscience.wiley.com).

ABSTRACT: Polypropylene/Ethylene–Octene copolymer (PP/EOC) blends were prepared by melt blending technique followed by compression molding. The effect of addition of EOC on the mechanical behavior of the PP matrix was investigated. Tensile and flexural strengths decreased with the incorporation of EOC. However, the impact strength of the matrix polymer increased in all the blend systems. The blends prepared at 30% EOC content showed an increase in the impact strength to the tune of 380% as compared with polypropylene (PP) matrix. The morphology of the fractured surfaces was investigated employing Scanning Electron Microscopy. SEM micrographs depicted the formation of biphase structure, wherein the EOC phases were homogeneously dispersed as small droplets within the PP matrix. WAXD patterns revealed that the α monoclinic form of isotactic PP does not show any significant change with the incorporation of EOC up to 70 wt %. DSC thermograms revealed a decrease in the melting temperature of the virgin matrix with the addition of EOC. The blend system at 50% EOC exhibited a broad crystallization exotherm at 75°C thus indicating multiple crystallization behavior primarily attributed to the difference in the nucleation process. Further DMA analysis showed presence of two different relaxation peaks corresponding to the T_g of EOC and PP matrix respectively, confirming the formation of a biphase structure. J Appl Polym Sci 104: 3137–3144, 2007

Key words: PP; EOC; mechanical; thermal properties; morphology; DSC; DMA; WAXD

INTRODUCTION

Polypropylene (PP) blends have received considerable importance in the recent years due to their low cost, easy processability combined with excellent mechanical, and thermal properties. These materials find tremendous potential for diversified end application in the field of packaging, automotives, and textiles etc. However high notch sensitivity, poor fractured toughness, and hardness of PP have been limiting factors for use in various engineering applications.[1–8]

Compounding of PP with a dispersed elastomeric phase i.e., ethylene–propylene–diene copolymer (EPDM), metallocene catalyzed polyethylene elastomer has been commonly practiced technique to alter stress distribution within the matrix and control crack propagation and termination.[9–15] The average size of the elastomer particles and their distribution within the matrix plays a vital role in influencing the overall properties of the blend. Significant improvement in toughness, thermal stability, and weld line strength with a simultaneous deterioration in stiffness and hardness with the inclusion of elastomeric phase have been reported by various authors.[16–19]

The development of metallocene catalyst has led to numerous new polyolefinic elastomer as toughening agent to improve low temperature performance of PP. This new class of PE modified by the nature of long chain branching and the arrangement of short chains in the macromolecule possesses a homogeneous copolymer distribution along with a narrow molecular weight distribution. Incorporation of these elastomers for the preparation of polyolefinic blends produces materials with easy processability and tailored properties for specific end use application.

In the present investigation an extensive study on the thermal and mechanical properties of PP/Ethylene–Octene copolymer (EOC) blends has been carried out as a function of different EOC loading to obtain optimum mechanical strength. The morphology of the PP/EOC blends were studied employing SEM to evaluate the extent of phase separation in the blends at the interfacial region. The blends were also subjected to DMA analysis to investigate the glass transition temperature, stiffness, and damping properties under periodic stress. Melting point and crystallization isotherm were also studied employing DSC measurements.

Correspondence to: S. K. Nayak (drsknayak@yahoo.com).

EXPERIMENTAL

Materials

Isotactic PP with a density of 0.9 g/cc and MFI of 11 g/10 min, obtained from Dow Chemicals, was used as the base polymer matrix.

Metallocene catalyzed EOC, Engage® 8180 with a density of 0.86 g/cc, MFI of 1 g/10 min and octene content of 25 wt %, obtained from Dow Elastomer, was used as the elastomer

Blending and specimen preparation

Blends of PP/EOC system containing different weight percentage of EOC: 0, 5, 10, 20, 30, 40, 50, 60, 70, 80, and 100% were prepared in a Torque Rheocord-9000 (Haake, Germany), with counter rotating roller rotor blades and a mixing chamber of 69 cm^3 volumetric capacity. The mixing was carried out at 190°C and 50 rpm for a period of 10 min. Subsequently, these premixes were homogenized on a two-roll mill (Collins, Germany), brought to room temperature and compression molded at 190°C using Delta Malikson 100 T press to produce sheets of 3 $\pm$ 0.1 mm thickness.

A contour cut copy milling machine, 6490 (Ceast, Italy), was used for the preparation of test specimens from the sheets as per ASTMD 638, ASTMD 790, and ASTMD 256 using calibrated templates.

Mechanical properties

Tensile strength

Specimens of virgin PP, EOC, and PP/EOC blends of dimensions 165 $\times$ 13 $\times$ 3 mm^3 were subjected to tensile test as per ASTM D-638, using Universal Testing Machine (UTM), LR-100K (Lloyd Instrument, U.K.). A crosshead speed of 50 mm/min and gauge length of 50 mm was used for carrying out the test.

Flexural strength

Specimens of virgin PP and PP/EOC blends having dimensions 80 $\times$ 12.7 $\times$ 3 mm^3 were taken for flexural test, under three point bending, using the same Universal Testing Machine in accordance with ASTM-D 790, at a cross head speed of 1.3 mm/min and a span length of 50 mm.

Impact strength

Similarly, Izod impact strength was determined from the specimens having dimensions 63.5 $\times$ 12.7 $\times$ 3 mm^3 with a ''V'' notch depth of 2.54 mm and notch angle of 450, as per ASTM-D 256, using Impactometer 6545 (Ceast, Italy).

For analyzing the mechanical properties, test specimens were initially conditioned at 23°C + 1°C and 55% + 2% RH. Five replicate specimens were used for each test and the data reported are the average of five tests. Corresponding standard deviations along with measurement uncertainty values for the experimental data showing the maximum standard deviation is also included.

Scanning electron microscopy analysis

The morphology of the impact fractured surfaces of virgin PP and PP/EOC blends were examined employing Scanning Electron Microscope JOEL JSM-5800, Japan. The samples were cryogenically fractured in liquid nitrogen and etched with heptane to extract the EOC phase for 7 days and then dried for $\approx$ 5 h at 80°C, followed by gold coating prior to study.

X-ray diffraction studies

Wide angle X-ray diffraction studies were carried out employing Philips X-ray generator and a Philips diffractometer (PW170 at 40 kV and 20 mA). A tube anode of Cu was used using $\lambda_1 = 0.15406$ and $\lambda_2 = 0.154439$ nm respectively. SAXS measurements were carried out employing Rigaku–Denki small angle chamber attached to Philips X-ray generator. Diffraction patterns were recorded at a scanning rate of 0.5 min/100 s using Ni - filtered radiation

Differential scanning calorimetry

The melting and crystallization behavior of virgin PP, EOC, and PP/EOC blends were studied employing Differential Scanning Calorimetry (Diamond DSC Perkin–Elmer). Samples of $\leq$ 5 mg weight were scanned from 40 to 200°C at a heating rate of 10°C/min to detect the melting characteristics of the virgin matrix and blend systems. For isothermal crystallization, the samples were heated from 40 to 200°C and held for 5 min at 200°C followed by cooling to 50°C at the rate of 10°C/min.

Dynamic mechanical analysis

Viscoelastic properties, such as storage modulus (E′), loss modulus (E″), and mechanical damping parameter (tan δ), as a function of temperature were measured in a Dynamic Mechanical Thermal Analyzer (VA 4000, Germany). The measurements were carried out in tensile mode using a rectangular specimen of dimensions 27.4 $\times$ 3.1 $\times$ 3 mm^3 over a temperature range of -100 to 150°C, at a heating rate of 3°C/min, under nitrogen flow. The samples were

TABLE I
Effect of Elastomer Loading on Tensile Properties of PP, EOC, and PP/EOC Blends

Elastomer (wt %)	Tensile strength (N/mm^2)	SD	Young's modulus (N/mm^2)	SD	Yield stress (N/mm^2)	SD
PP (Virgin)	19.37	0.56	509.0	0.48	18.90	0.69
5	17.48	0.71	413.0	0.51	16.39	0.71
10	14.47	0.85	256.4	0.49	11.85	0.83
20	13.02	0.83	197.6	0.57	13.10	0.91
30	8.28	0.87	107.0	0.65	8.54	0.99
40	6.32	0.93	96.4	0.69	6.31 ± 1.47	1.24
50	5.29	0.97	82.4	0.89	4.47	1.01
60	6.72 ± 1.35[a]	1.12	45.2	1.03	3.46	1.12
70	6.47	1.01	12.2 ± 1.37	1.28	2.23	1.03
80	6.07	0.99	5.3	1.11	2.04	0.96
EOC (virgin)	7.33	0.63	1.7	0.61	1.86	0.70

[a] Measurement uncertainty values as per A2LA guidelines[44] incase of the experimental data showing the maximum standard deviation. SD, Standard deviation.

scanned at a fixed frequency of 10 Hz, with a static strain of 0.2% and dynamic strain of 0.1%.

RESULTS AND DISCUSSION

Mechanical properties

Tensile properties

The effect of blend composition on the tensile properties of PP/EOC system is represented in Table I. It is evident from the test results that with the increase in EOC content, there is a decrease in tensile strength and Young's modulus as compared with virgin PP. This decrease in tensile strength and Young's modulus of PP virgin, with the addition of 30% EOC were found to be 57 and 79% respectively, which is primarily due to the presence of soft elastomeric phase that reduces the crystallinity and stress level of the virgin PP to produce shear yielding.[20] The yield strength of PP also decreased with a progressive increase in EOC content, thus revealing immiscibility of the components with the formation of a biphase structure.[21] However all the blends exhibited high elongation (>300%) and the specimens showed no break under the testing conditions. Similar observations have also been reported by Premphet and Paechareonchai[22] for PP/Metallocene catalyzed EOC blends. Simanke et al.[23] have investigated that an increase in the comonomer content impede the crystallization of polymer chains thereby resulting in decrease in tensile strength and modulus of the copolymer. Similar results are observed in the present investigations.

Flexural properties

The variation of flexural properties of PP/EOC blends as a function of EOC content is enumerated in Table II. As implied from the test results, there is a sequential decrease in flexural strength and flexural modulus with the incorporation of EOC into PP matrix. This behavior is probably due to the formation of pores by the elastomer phase at the interface region. The presence of elastomer in the blends linearly reduces the stiffness of the virgin polymer due to an associated reduction in the effective cross-sectional area of the sample as investigated by Lotti and Canevarolo[24].

Impact strength

The effect of EOC content on notched Izod impact strength of various PP/EOC blends at room temperature is depicted in Figure 1. The curves depict two transition regions. At low EOC content of less than 15 wt % a marginal increase in the impact strength was observed. Experimental findings revealed, brittle characteristics of the virgin matrix with an impact strength of about 114 J/m. Incorporation of elastomeric phase leads to an increase in the impact

TABLE II
Effect of Elastomer Loading on Flexural Properties of PP, EOC, and PP/EOC Blends

Elastomer (wt %)	Flexural strength (N/mm^2)	SD	Flexural modulus (N/mm^2)	SD
PP (Virgin)	60.71 ± 0.95	0.78	805.9	0.93
5	57.08	0.93	781.6 ± 1.2	1.08
10	49.42	0.81	678.7	0.83
20	23.46	0.89	560.2	0.89
30	14.70	0.82	281.8	0.88
40	12.26	0.78	146.6	0.87
50	–		–	
60	–		–	
70	–		–	
80	–		–	
EOC (virgin)	–		–	

The flexural strength & modulus of the blends at 50, 60, 70, and 80% loading of EOC and virgin EOC could not be expedited due to higher content of elastomeric phase.

strength of the matrix polymer. The blend prepared incorporating 30% EOC showed optimum performance with an increase of about 380% in impact strength as compared with virgin PP. This phenomenal transition from brittle to ductile behavior is probably due to the presence of smaller elastomeric domains, which are effectively dispersed within the PP matrix, thereby leading to dissipation of more impact energy[25]. Many explanations have been proposed governing the brittle to ductile transitions in the blends. Wu[26] have demonstrated that the distance between the rubber particles or matrix ligament thickness have been the key parameter in governing the toughening mechanism in the blends. Regardless of particle size and rubber concentration, the blend is tough if the matrix ligament thickness is kept lower than a critical value.[26,27] Ligament thickness value of approximately 0.3 and 0.6 μm have been reported for polyamide 66 and polyethylene respectively. However, brittle–ductile transition as measured by notched izod impact strength for PP/EPR blends, cannot be described with a ligament thickness parameter as per Vander Waals observation. Hence, the dependence of toughening efficiency on the spatial distribution have been investigated to be stronger than the matrix ligament thickness.[28,29]

However, beyond 30% EOC content a decline in the impact strength of the blends was observed. This behavior is probably due to high EOC content which results in poor dispersion within the PP matrix whereas at low EOC content it was possible to obtain blends with smaller rubber particles well dispersed in the continuous matrix.[25] Furthermore higher EOC content probably leads to phase separation which contributes to a decrease in the impact energy.

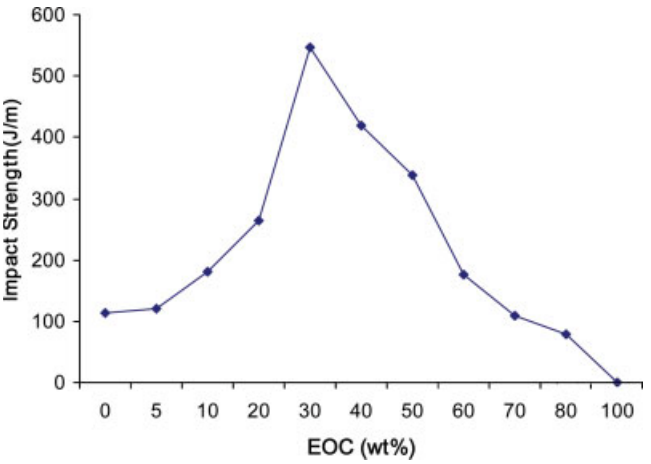

Figure 1 Effect of EOC loading on the impact strength of PP/EOC blends.

Scanning electron microscopy analysis

The SEM micrographs of the impact fractured surfaces of virgin PP and PP/EOC blends are illustrated in Figure 2(a–d) respectively. In case of virgin PP, a relatively smooth surface was observed which revealed brittle fracture behavior of the matrix polymer. The phase separation between the PP phase and the EOC rich phase is clearly observed at 30% EOC content [Fig. 2(b)], which is generally used to improve the low temperature impact strength of PP. The elastomer formed small particles with the appearance of droplets finely distributed in the continuous matrix of PP. The phases also reveal good adhesion due strong interaction of the amorphous phase in EOC and that in as reported in other PP/elastomer blends.[30] At higher EOC content of 70% [Fig. 2(d)], the elastomer forms the matrix with PP droplets dispersed in it. It appears that phase inversion takes place at an intermediate blend ratio. Figure 2(c) depicts the blend morphology at an intermediate blend ratio wherein it is expected to achieve a continuous phases between both the components. However, closer examination of the structure reveals regions with different compositions and different continuous phases. In some areas, EOC forms the continuous phase with occluded PP droplets while there are regions where PP is the continuous matrix containing EOC islands. Similar kind of transitional morphology has also been reported by Yingwei et al.[30] The state of dispersion in a heterogeneous blend system is determined by the rheological properties of the constituent components and processing conditions under which the blends are prepared that further defines the size, shape, and distribution of various blend constituents.[25] These facts shall be elaborately discussed in our future investigations.

A regular dual continuity structure is rarely attainable final form of the morphology. Although the transitional morphology is hard to define precisely in our present investigation, a completely dispersed structure is detected below 30% and above 70% of EOC content. This can be substantiated with the evidence of the coexistence of continuous and dispersed phases. PP phases revealed with the appearance of two peaks in the crystallization exotherms [Fig. 5(c)]. Furthermore, at 70 wt % of EOC content, the primary PP crystallization peak disappeared thus showing a completely dispersed PP phase. Also a maximum in the amount and melting peak temperature of β PP was observed at 30% EOC content. This further confirms that the compositions where transitions take place are in between 30 and 70 wt % of EOC and that dispersed morphology results in different crystallization and melting for the PP/EOC blends used in this study. The micrographs revealed a coarser appearance in all the blends studied.

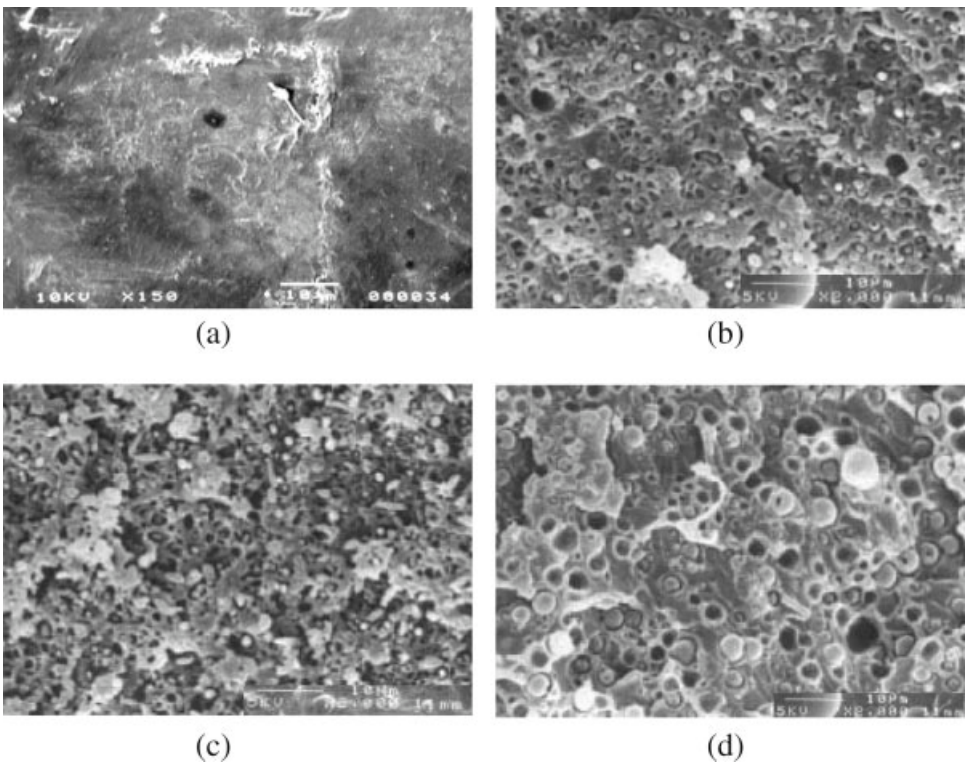

Figure 2 (a) SEM Micrograph of PP virgin at a magnification of 10 μm; (b) SEM Micrograph of PP/30% EOC blends at a magnification of 10 μm; (c) SEM Micrograph of PP/50% EOC at a magnification of 10 μm; (d) SEM Micrograph of PP/70% EOC virgin at loading at a magnification of 10 μm.

Characterization

X-ray diffraction studies

Isotactic PP crystallizes primarily in three different forms; α monoclinic, β̃ pseudohexagonal and γ orthorhombic respectively. The most common form is α monoclinic with β and γ type formed under specific conditions. β̃ form crystal is generally formed by monitoring the quenching conditions or addition of suitable nucleating agents[30,31] whereas γ form appears primarily in presence of short polymer chains or in case of a copolymer with small amount of ethylene or by conducting crystallization process under high pressure.[32] In the present investigation wide angle X-ray diffraction (WAXD) patterns of virgin PP and PP/EOC blends represented in Figure 3, reveals α monoclinic form around 18°–19°, β̃ pseudohexagonal peak at 16°–17° and γ orthorhombic at 19°–21° respectively. As evident from the WAXD patterns the α monoclinic form of isotactic PP does not show any significant change with the incorporation of EOC up to 70 wt %. These results can be further corroborated with DSC thermograms.

Differential scanning calorimetry analysis

DSC heating and cooling thermograms, illustrating melting and crystallization behavior of EOC, virgin PP, and PP/EOC blend system is depicted in Figures 4 and 5 respectively. DSC curves were normalized by mass and shifted to permit better visualization of the transition peaks. It is evident that the thermograms (Fig. 4) show a single endothermic peak, characteristic melting transition of α PP around 167°C. The blends also reveal similar melting range of PP matrix. No melting was detected at a lower tempera-

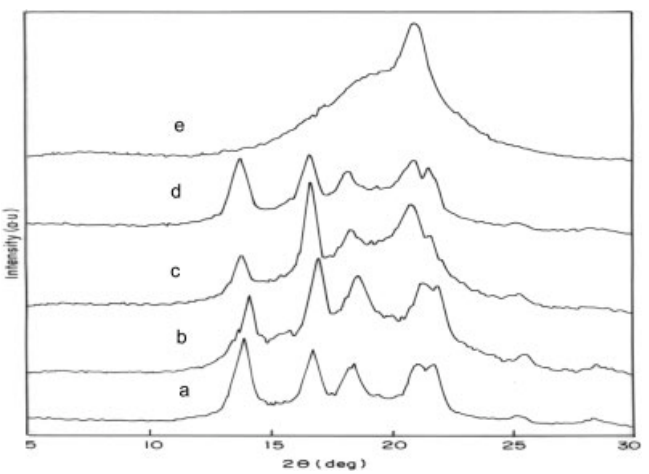

Figure 3 WAXD patterns of (a) virgin PP (b) PP/30% EOC blend (c) PP/50% EOC blend (d) PP/70% EOC blend (e) virgin EOC.

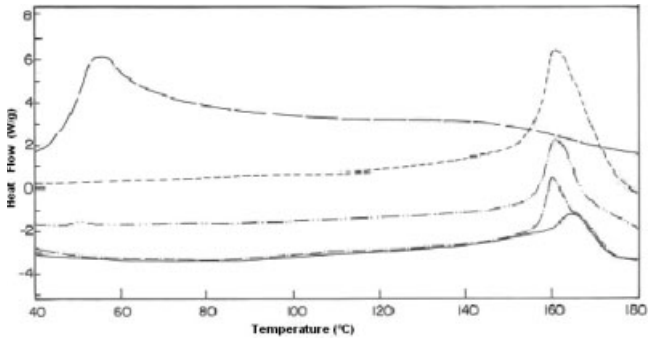

Figure 4 DSC melting thermogram of (a) virgin PP (b) PP/30% EOC blend (c) PP/50% EOC blend (d) PP/70% EOC blend (e) Virgin EOC.

ture which further confirms the existence of pseudo-hexagonal modification of iPP in the blends.[30] However, the blends prepared at 70% EOC content reveals a wide melting temperature at lower temperature around 50°C. This is probably due to incomplete miscibility of PP and EOC at high EOC content. This phenomenon also shows that the elastomer EOC at 70 wt % acts as a nucleating agent to promote the formation of a β crystalline form under slow cooling rate. Similar phenomenon has been observed by Yingwei et al.[30] at 50 : 50 ratio of PP/E1801 blends. However, as reported by the workers no unambiguous explanation has been found for this phenomenon up to now.

Melting temperature of crystalline polymers can be related to the size and perfection of crystal units. The melting (T_m) and crystallization temperature (T_c), and enthalpy of fusion ΔH_f are represented in Table III. As evident from Figure 4 and Table III, the melting peak decreased marginally with elastomeric addition, which indicates a small decrease in lamellar thickness. This further concludes that incorporation of EOC, results in decrease in size and perfection of PP crystals and increase in amorphous regions between the lamellae thus inhibiting the

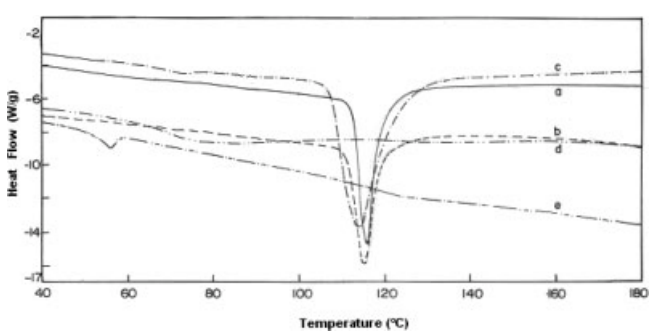

Figure 5 Crystallization thermogram of (a) virgin PP (b) PP/30% EOC blend (c) PP/50% EOC blend (d) PP/70% EOC blend (e) Virgin EOC.

TABLE III
Thermal Properties of PP, EOC, and PP/EOC Blends

Elastomer (wt %)	T_m (°C)	T_c (°C)	ΔH_f^{obs} (J/g)
0	165	115	70
30	162	114	49
50	161	113	34
70	161	90	21
100	58	55	–

T_c, Crystallization temperature.
T_m, Melting temperature.

crystallization process of PP. In case of virgin EOC, a melting peak of ≈ 58°C was noticed thus indicating a certain degree of crystallinity.

Furthermore, it was also observed that there was a sequential decrease in the ΔH_f^{obs} with the incorporation of elastomeric phase. This is primarily due to decrease in the PP content in the blends.

The DSC crystallization exotherms of virgin PP, EOC, and PP/EOC blend systems is enumerated in Figure 5. DSC crystallization exotherms were also normalized by mass and shifted to permit better visualization of the peaks. It is evident that the PP and the blend containing 30% EOC revealed a single crystallization peak around 118°C. However for the blend system prepared at 50% EOC, the DSC thermogram exhibited a broad crystallization peak around 75°C. This phenomenon of multiple crystallization behavior is primarily attributed to the difference in the nucleation process.[30] These findings are analogous to the results of classical droplet crystallization in which crystallization is inhibited until heterogeneous nucleation occurs.[33] Hence the presence of a crystallization exotherm of PP at 75°C is probably due to crystallization by homogenous nucleation.[30] Polymer blends showing multiple crystallization behavior have been widely reported by various authors.[34–35] Ghijsels et al.[36] have reported that an increase in elastomer content in PP/styrene–butadiene thermoplastic blends results in a change in morphology and crystallization process. At a certain elastomer content, the elastomer forms the continuous phase with dispersed PP droplets resulting in homogeneous nucleation. Decrease of the heterogeneous nucleation was also observed by Chun et al.[37] for PP/PC blends in which homogeneous nucleation of PP in PC rich composition was found more dominant than the heterogeneous nucleation when PP forms the dispersed droplets.

At 70 wt % of EOC, the crystallization of PP at high temperature was not observed. This is probably for the reason that PP becomes completely dispersed in EOC matrix and homogeneous nucleation dominates the nucleation process of PP matrix. Further, the crystallization exotherm of virgin EOC (Fig. 3) revealed a peak around 55°C.

Dynamic mechanical analysis

The temperature dependence of storage modulus (E′), and damping parameter (tan δ) of PP, EOC, PP/EOC and is depicted in Figures 6 and 7 respectively. It is evident that E′ of the virgin matrix decreases with the incorporation of elastomeric phase. This decline in storage modulus of PP matrix is primarily due to the presence of soft elastomeric phase, which reduces the crystallinity and stress level of the virgin matrix. Further the DMA results can be correlated with the decrease in flexural modulus with the incorporation of EOC. In all the cases, E′ decreased with the increase in temperature.

PP showed three relaxation peaks −80°C(γ), 8°C (β), and 100°C(α) respectively. The temperature of the β relaxation maximum corresponds to the T_g of the matrix, while the α relaxation peak is related to the slip mechanism in the crystallites. The γ relaxation peak is due to the motion of the small chain groups like methyl and methylene.[37,38] In the present investigation, the tan δ curve of PP showed two relaxation peaks at temperature around 10 and 80°C respectively. The low temperature β peak is associated with the T_g in the amorphous regions while the high temperature α peak corresponds to intracrystalline chain motion.[39–41] Virgin EOC exhibited a more accentuated relaxation peak between −50°C and −40°C, which is probably due to micro Brownian motion of amorphous chains.[42] In case of the blends containing 30 and 50% EOC, the tan δ curve showed two peaks at −50°C to −40°C and around ≈ 10°C respectively. The high temperature relaxation peak is probably associated with the T_g of amorphous region of PP and lower relaxation peak corresponds to T_g of EOC.[43] This further confirms that with the incorporation of elastomeric phase, the blends showed two different peaks corresponding to the T_g's of individual components confirming the formation of a biphase structure. However, in case of the blends containing 70% EOC, the T_g corresponding to the elastomer at −50°C to −40°C was observed, which is probably due to EOC rich phase.

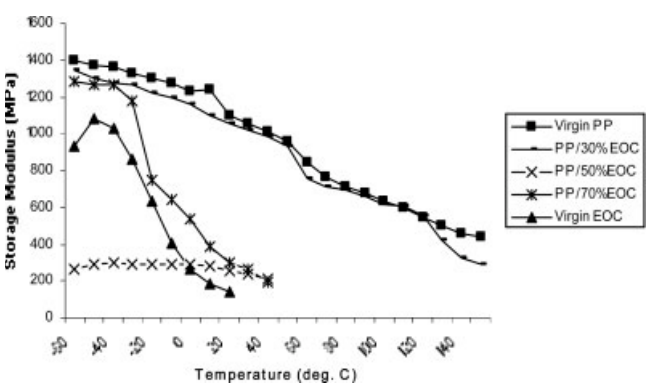

Figure 6 Variation of E′ of Virgin PP, Virgin EOC and the blends with temperature.

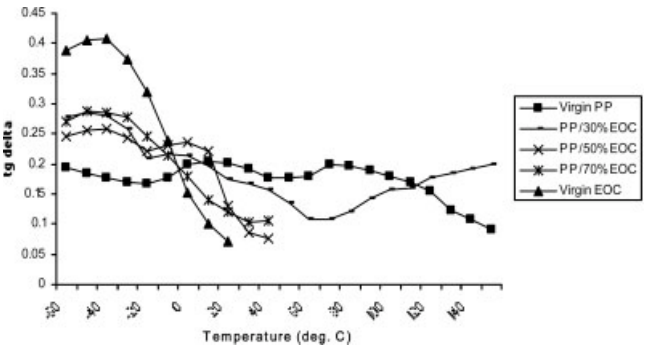

Figure 7 Variation of tan δ of Virgin PP, Virgin EOP and the blends with temperature.

CONCLUSIONS

The mechanical and dynamic mechanical properties of PP/EOC blend systems have been investigated. It was observed that the tensile and flexural properties of the virgin matrix decreased with the incorporation of EOC. However, there was a substantial increase in the impact strength of PP virgin to the tune of 370% at 30% EOC loading. Storage modulus versus temperature plots also showed a decreased in the magnitude of the peaks in the blend systems. Tan δ curve exhibited two relaxation peaks at temperatures corresponding to the T_g of individual components thus revealing formation of a biphase structure in the blends. WAXD patterns revealed that α monoclinic form of isotactic PP does not show any significant change with the incorporation of EOC up to 70 wt %. DSC thermograms further indicated a decrease in the crystallinity of the matrix polymer with the addition of EOC. Further, morphological findings showed extensive plastic deformation with a homogenized dispersion of EOC phases within the PP matrix.

References

1. Bailey, M. S.; Brauer, D. Mod Plast 1993, 11, 12.
2. Gupta, A. K.; Ratnam, B. K.; Srinivasan, K. R. J Appl Polym Sci 1992, 45, 1303.
3. Randall, J. C. (to Exxon Chem). E.P.O. Pat. 351,208 (1990).
4. Silva, A. L. N.; Coutinho, F. M. B.; Rocha, M. C. G. Plast Mod 1996, 40, 264.
5. Borruso, A. V. Presented at TECHNON Petrochemical Seminar, Rio de Janeiro, Brazil, 1994.
6. Silva, A. L. N.; Coutinho, F. M. B.; Rocha, M. C. G.; Tavares, M. I. B. J Appl Polym Sci 1997, 66, 2005.
7. Kal, L. T.; Plumley, T. A.; Patel, R. M.; Jain, P. ANTEC 1995, 2249.
8. Lai, S.; Plumley, T. A. ANTEC 1994, 1814.
9. Long, Y.; Shanks, R. A. J Appl Polym Sci 1996, 61, 1877.
10. Danesi, S.; Porter, R. S. Polymer 1978, 19, 448.

11. Kim, B. K.; Do, I. H. J Appl Polym Sci 1996, 61, 439.
12. Petrovic, Z. S.; Budinski-Simendic, T.; Divjakovic, V.; Skrbic, Z. J Appl Polym Sci 1996, 59, 301.
13. Lemstra, P. J.; Meijer, H. E. H.; Van Gisbergen, J. G. M. Polymer 1989, 30, 2153.
14. Dao, K. C. Polymer 1984, 25, 1527.
15. Inoune, J.; Suzuki, T. J Appl Polym Sci 1995, 56, 1113.
16. Van der Waal, A.; Verheul, A. J. J.; Gaymans, R. J. Polymer 1999, 40, 6057.
17. Margolina, A.; Wu, S. Polymer 1988, 29, 2170.
18. Borggreve, R.; J. M.; Gaymans, R. J.; Schuijer, J.; Ingen Housz, J. F. Polymer 1987, 28, 1489.
19. Speri, W. M.; Patrick, G. R. Polym Eng Sci 1975, 15, 668.
20. Jang, B. Z.; Uhlmann, D. R.; Vander Sande, J. B. J Appl Polym Sci 1985, 30, 2485.
21. Da Silva, A. L. N.; Coutinho, F. M. B.; Rocha, M. C. G.; Bretas, R.; Scuracchio, C. J Appl Polym Sci 2000, 75, 692.
22. Premphet, K.; Paechareonchai, W. J Appl polym Sci 2002, 85, 2412.
23. Simanke, A. G.; Galland, G. B.; Neto, R. B. H.; Quijada, R.; Mauler, R. S. J Appl Polym Sci 1999, 74, 1194.
24. Lotti, C.; Canevarolo, S. V. Polym Test 1998, 17, 523.
25. Lopez-Manchado, M. A.; Valle, M.; Sapunar, R.; Quijada, R. J Appl Polym Sci 2004, 92, 3008.
26. Wu, S. Polymer 1985, 26, 1855.
27. Wu, S. Polymer 1988, 35, 549.
28. Liu, Z. H.; Zhang, X. D.; Zhu, X. G.; Qi, Z. N.; Wang, F. S.; Li, R. K. Y.; Choy, C. L. Polymer 1998, 39, 5027.
29. Liu, Z. H.; Zhang, X. D.; Zhu, X. G.; Qi, Z. N.; Wang, F. S.; Li, R. K. Y.; Choy, C. L. Polymer 1998, 39, 5047.
30. Yingwei, Di.; Iannace, S.; Nicolais, L. J Appl Polym Sci 2002, 86, 3430.
31. Busse, K.; Kressler, J.; Maier, R.; Scherble, J. Macromolecules 2000, 33, 8775.
32. Angelloz, C.; Fulchiron, R.; Douillard, A.; Chabert, B. Macromolecules 2000, 33, 4138.
33. Wundelich, B. Macromolecular Physics; Academic Press: New York, 1976; Vol. 2.
34. O'Malley, J. J.; Crystal, R. G.; Erhardt, P. F. Block Copolymer; Plenum: New York, 1970.
35. Aref-Azar, A.; Hay, J. N.; Marsden, B. J.; Walker, N. J Polym Sci Part B: Polym Phys 1980, 18, 637.
36. Ghijsels, A.; Groesbeek, N.; Yip, C. W. Polymer 1982, 23, 1913.
37. Chun, Y. S.; Jung, H. C.; Han, M. S.; Kim, W. N. Polym Eng Sci 1999, 39, 2304.
38. Botev, M.; Betchev, H.; Bikaris, D.; Panayiotou, C. J Appl Polym Sci 1999, 74, 523.
39. Dumoulin, M. M.; Utracki, L. A. Polym Eng Sci 1987, 20, 167.
40. Boyd, R. H. Polymer 1985, 56, 323.
41. Ashcraft, C. R.; Boyd, R. H. J Polym Sci Polym Phys Ed 1976, 14, 2153.
42. Silva, A. L. N.; Rocha, M. C. G.; Coutinho, F. M. B.; Bretas, R.; Scuracchio, C. J Appl Polym Sci 2001, 79, 1634.
43. Gao, J.; Wang, D.; Yu, M.; Yao, Z. J Appl Polym Sci 2004, 93, 1203.
44. Adams Thomas, M. A2LA guidelines for estimation of measurement uncertainty in testing; The American Association for Laboratory Accreditation: Frederick, MD, 2002; p 1.